Elena Costariol ORCID iD: 0000-0002-3801-5684

Qasim Rafiq ORCID iD: 0000-0003-4400-9106

Establishing the scalable manufacture of primary human T-cells in an automated stirred-tank bioreactor

Elena Costariol[1], Marco Rotondi[1], Arman Amini[1], Christopher J. Hewitt[2], Alvin W. Nienow[2,3], Thomas R.J. Heathman[4], Martina Micheletti[1] and Qasim A. Rafiq[1*]

[1]Advanced Centre for Biochemical Engineering, Department of Biochemical Engineering, University College London, London, WC1E 6BT, United Kingdom

[2]Aston Medical Research Institute, School of Life and Health Sciences, Aston University, Birmingham, B4 7ET, United Kingdom

[3]School of Chemical Engineering, University of Birmingham, Edgbaston, Birmingham, B15 2TT United Kingdom

[4]Hitachi Chemical Advanced Therapeutic Solutions (HCATS), 4 Pearl Court, Allendale, NJ, 07401

*Correspondence: Dr Qasim Rafiq, Advanced Centre for Biochemical Engineering, Department of Biochemical Engineering, University College London, Gower Street, London, WC1E 6BT, United Kingdom

E-mail: q.rafiq@ucl.ac.uk

Short running title: Scalable manufacture of T-cells in a STR

Keywords: Immunotherapy; Bioprocessing; Manufacture; Stirred-tank Bioreactor; Scale-up; T-cell.

Abstract

Advanced cell and gene therapies such as chimeric antigen receptor T-cell immunotherapies (CAR-T), present a novel therapeutic modality for the treatment of acute and chronic conditions including acute lymphoblastic leukaemia and non-Hodgkin lymphoma. However, the development of such immunotherapies requires the manufacture of large numbers of T-cells which remains a major translational and commercial bottleneck due to the manual, small-scale and often static culturing systems used for their production. Such systems are used because there is an unsubstantiated concern that primary T-cells are shear sensitive, or prefer static

This article has been accepted for publication and undergone full peer review but has not been through the copyediting, typesetting, pagination and proofreading process, which may lead to differences between this version and the Version of Record. Please cite this article as doi: 10.1002/bit.27088.

conditions, and therefore do not grow as effectively in more scalable, agitated systems, such as stirred-tank bioreactors, as compared to T-flasks and culture bags. In this study, we demonstrate, that not only can T-cells be cultivated in an automated stirred-tank bioreactor system (ambr® 250), but that their growth is consistently and significantly better than that in T-flask static culture, with equivalent cell quality. Moreover, we demonstrate that at progressively higher agitation rates over the range studied here, and thereby higher specific power inputs (P/M W kg^{-1}), the higher the final viable T-cell density; i. e., a cell density of 4.65 ± 0.24 x 10^6 viable cells ml^{-1} obtained at the highest P/M of 74 x 10^{-4} W kg^{-1} in comparison to 0.91 ± 0.07 x 10^6 viable cells ml^{-1} at the lowest P/M of 3.1 x 10^{-4} W kg^{-1}. We posit that this improvement is due to the inability at the lower agitation rates to effectively suspend the Dynabeads®, which are required to activate the T-cells; and that contact between them is improved at the higher agitation rates. Importantly, from the data obtained, there is no indication that T-cells prefer being grown under static conditions or are sensitive to fluid dynamic stresses within a stirred-tank bioreactor system at the agitation speeds investigated. Indeed, the opposite has proven to be the case, whereby the cells grow better under higher agitation speeds whilst maintaining their quality. This study is the first demonstration of primary T-cell *ex vivo* manufacture activated by Dynabeads® in an automated stirred-tank bioreactor system such as the ambr® 250 and the findings have the potential to be applied to multiple other cell candidates for advanced therapy applications.

Graphical Abstract

Advanced cell and gene therapies such as chimeric antigen receptor T-cell immunotherapies (CAR-T), present a novel therapeutic modality for the treatment of acute and chronic conditions including acute lymphoblastic leukaemia and non-Hodgkin lymphoma.

Baffled Vessel		
Impeller diameter (3-pitched blade) (D)	26 mm	T/D = 2.3
Impeller height from bottom (C)	17 mm	C/D = 0.65
Impeller number	2	
Impeller spacing	30 mm	
No. of baffles	4	
Baffle width (W)	6.25 mm	W/T = 0.1

Baffled Vessel (two impellers)

Unbaffled Vessel		
Impeller diameter (Elephant ear) (D)	30 mm	T/D = 2
Impeller height from bottom (C)	17 mm	C/D = 0.56
Impeller number	1	
No. of baffles	0	

Unbaffled Vessel (single impeller)

Introduction

The emergence of novel cell and gene-modified therapies (CGTs) has generated significant commercial and clinical interest owing to their demonstrable efficacy. This interest is reflected by the increasing number of clinical trials using this therapeutic modality (over 300 reported), and over $2.1 billion raised in global financing for gene and gene-modified cell therapies (Alliance for Regenerative Medicine, 2018). More importantly, however, is the growing number of CGTs receiving regulatory approval by the US FDA and EMA enabling such therapies to be adopted and enter routine clinical practice (EMA, 2018a, 2018b, 2018c; FDA, 2019). The most prominent example is that of the engineered chimeric antigen receptor (CAR) T-cell products which has demonstrated significant clinical efficacy, most notably against non-Hodgkin lymphoma and paediatric B-cell acute lymphoblastic leukemia. These therapies have not only obtained regulatory approval but will be reimbursed by both private healthcare insurers and national social healthcare systems (NHS England, 2018).

Yet despite the clinical success of Novartis' Kymriah™ (tisagenlecleucel) and Gilead's Yescarta™ (axicabtagene ciloleucel) CAR-T products, the cost-effective, reproducible and robust manufacture of such therapies remains a significant translational and commercial bottleneck, with manufacturing failures as high as 9% of commercial doses (BioPharma Dive, 2018). With the price of such therapies in excess of $300,000 (Business Insider, 2018), it is necessary to address the underlying manufacturing issues associated with personalized therapies. CGT manufacturing processes tend to be open in nature which therefore necessitates the use of expensive cleanroom facilities. Moreover, many processes involve manual steps requiring highly skilled and experienced operators which can lead to errors, product variation and potentially, contamination. These factors contribute to the significant cost of manufacturing these advanced therapies, and if addressed, will lower the cost of production and enable CGTs to be widely accessible to a global population.

The current production of CAR-T therapies typically involves the isolation of patient material *via* leukapheresis, followed by cell selection, T-cell activation (often using magnetic Dynabeads® covalently coupled to anti-CD3 and anti-CD28 antibodies to mimic the role of antigen-presenting cells), transduction of the T-cells to express the CAR using a viral vector or non-viral method, and expansion of the transduced cells prior to final formulation (Wang & Rivière, 2016). The open and manual nature of the current CAR-T manufacturing process results in significant operational and capital expenditure due to the aforementioned reasons. Moreover, as patient numbers increase, a significant burden will be placed on current production platforms. These platforms were not designed to treat large patient cohorts and therefore multiple patient cell processing and scalability of autologous CGT therapies remains a significant bottleneck. To facilitate the production of individualized, patient-specific CGT products, high-throughput, automated and robust expansion technologies are required (Klarer et al., 2018). As efforts are made toward establishing 'off-the-shelf' allogeneic CAR-T therapies using gene editing tools (Gouble et al., 2014) or peptides (Celyad, 2018), the development of large-scale manufacturing systems becomes critical and requires the use of controlled bioreactor platforms.

Nevertheless, the production of primary T-cells has often been considered optimal under static conditions despite the cells being a suspension cell type by nature, with many clinical and small-scale processes opting to employ static T-flask or sterile culture bags for cell production (Vormittag et al., 2018). Such systems are inherently inefficient and result in culture conditions which are heterogeneous and uncontrolled with respect to dO_2 and pH. To overcome these challenges, clinical research and commercial groups have employed the use of rocking motion bioreactor systems (e.g. GE Healthcare's WAVE® bioreactor or BIOSTAT® RM from Sartorius Stedim Biotech) which improve the homogeneity of the culture, sampling and implementation of process control strategies (Marsh et al., 2017; Vormittag et al., 2018). These developments have demonstrated that T-cells can be grown in a non-static environment but little work has been done in stirred-tank bioreactors. Some early work was successful

in demonstrating the growth of T-cells in both spinner flasks and small bioreactors (Carswell and Papoutsakis, 2000; Bohnenkamp et al., 2002) but neither used Dynabeads® for cell activation. Surprisingly, further work does not seem to have been undertaken since then. This lack of activity is likely due to the common unsubstantiated concern that such cells are too fragile to withstand the fluid dynamic environment found in stirred-tank bioreactors. However, there have been extensive studies in the literature which have demonstrated the potential to culture numerous mammalian and human cells under both transitional and turbulent fluid dynamic conditions for both free suspension cells (Nienow, 2006) and adherent cells on microcarriers (Chen et al., 2015; Nienow et al., 2016; Rafiq et al., 2013b; Rafiq et al., 2017).

In any case, stirred-tank bioreactors are the workhorse of the biologics industry, where suspension CHO cells are cultured to produce monoclonal antibodies (Nienow, 2015; Rafiq & Hewitt, 2015); and they are becoming more so for the cultivation of human mesenchymal stem cells (hMSCs) and human pluripotent stem cells on microcarriers (Carmelo et al., 2015; Heathman et al., 2015; Rafiq et al., 2013c). Given the significant advantages of stirred-tank bioreactor systems over other expansion platforms (Rafiq et al., 2016b), not least the proven scalability, extensive engineering and biological characterisation, and process monitoring and control capability, the present study aims to demonstrate the growth of primary T-cells from multiple healthy donors in agitated, stirred-tank bioreactor environments.

The simplest stirred bioreactor is the spinner flask; whilst these systems are uncontrolled with respect to dO_2 and pH, it is often the first step for culturing new cell types in a mechanically agitated environment. It is therefore a suitable place to start investigating the possibility of using stirred bioreactors with T-cells especially as the platform has proved particularly useful in establishing the cultivation of human mesenchymal stem cells on microcarriers in stirred systems (Hewitt et al., 2011; Rafiq et al., 2013a) amongst other cell types (Badenes et al., 2017; Diogo et al., 2015). Other, more advanced, small scale systems include automated stirred bioreactor platforms such as the ambr® 15 (Nienow et al., 2013a; Rafiq et al., 2017) and ambr® 250.

In this work, the growth of primary T-cells from three healthy human donors was investigated in spinner flasks and in the ambr® 250, multi-parallel, stirred-tank bioreactor system. The ambr® 250 provides extensive process monitoring and control capability which far exceeds that of existing T-flask, culture bag-based or spinner flask systems. Moreover, the operation of the individual bioreactors within the ambr® 250 platform can be fully automated and enables the simultaneous operation of up to 24 individual bioreactors in parallel, each with a maximum working volume of 250 ml. Thus it seems a very suitable system to use to investigate the potential of stirred bioreactors for cultivating primary T-cells. It also presents a potentially scalable manufacturing platform for autologous CGTs (i.e. scale-out rather than scale-up) with cell culture volumes unlikely to exceed the need for >200 ml. Additionally, such platforms have significant value as scale-down models for high-throughput screening and optimisation of culture parameters and reagents, particularly as allogeneic CAR-Ts emerge as a potential therapeutic modality. Ultimately, the study will explore whether stirred-tank bioreactors can be used as a standard system for manufacturing CAR-T cell products, complementing and potentially replacing the existing technologies.

Materials and Methods

T-cell isolation and pre-expansion

Fresh peripheral blood mononuclear cells (PBMCs) from three healthy human donors were purchased from Cambridge Bioscience (Cambridge Bioscience, UK). All donors provided appropriate consent and the studies undertaken were approved by the local Ethics Committee. T-cells from the three donors

were isolated from the PBMC samples using the Pan T Cell Isolation Kit (Milteny Biotec Ltd., UK) combined with LS Columns (Milteny Biotec Ltd., UK) following the manufacturer instructions. The cells were cryopreserved at $1x10^7$ cells ml^{-1} in 1 ml of CryoStor® CS10 (STEMCELL Technologies UK Ltd, UK). All cell culture studies (T-flask, spinner flask and ambr® 250 bioreactor) involved culturing cells in Roswell Park Memorial Institute (RPMI) 1640 Medium (Gibco® Thermo Fisher Scientific, Loughborough, UK) supplemented with 10% FBS (Thermo Fisher Scientific, UK), 2mM L-Glutamine (Thermo Fisher Scientific, UK) and 30 IU ml^{-1} Interleukin-2 (IL-2) (Milteny Biotec Ltd., UK). Cells were seeded at $1x10^6$ cells ml^{-1}, activated using a 1:1 ratio of cells to Magnetic Dynabeads® (Thermo Fisher Scientific, UK) and expanded in T-175 flask at 37°C and 5% CO_2 in a humidified incubator. The superparamagnetic Dynabeads® are approximately 4.5 µm in diameter and have covalently coupled anti-CD3 and anti-CD28 antibodies designed to replicate the normal series of events by which T cells are activated. T-cell activation is important as this facilitates proliferation, without which, cell growth would be poor. Complete medium was added to the cells every 2-3 days in order to maintain cell density in the range of 1- 3 x 10^6 cells ml^{-1}. The cells were expanded for 7 days in order to obtain a sufficient cell number for the spinner flask (25 x 10^6 cells) and ambr® 250 bioreactor (50 x 10^6 cells per vessel) experiments. The cells were not frozen following the pre-expansion step, rather, were inoculated directly into the expansion platforms.

Spinner flask culture

Reusable, glass spinner flasks (BellCo, USA), with a vessel height and diameter of 135 mm and 60 mm respectively, was fitted with a magnetic horizontal stirrer bar (40 mm length) and a vertical paddle (50 mm diameter) and was used for all spinner flask experiments. The horizontal magnetic stir bar was set approximately 5 mm above the dimpled bottom of the spinner flask to ensure fluid flow was not impeded. Prior to culture, the spinner flasks were autoclaved and inoculated in a Class 2 biosafety cabinet (BSC). The spinner flasks were placed on a BellEnnium™ Compact 5-position magnetic stirrer platform (BellCo, USA) in a humidified incubator at 37°C and 5% CO_2 and set to agitate at 35rpm, the agitation speed at which multiple spinner flask experiments have been undertaken with hMSCs which are also perceived to be 'shear sensitive'(Hewitt et al., 2011; Nienow et al., 2014; Rafiq et al., 2016a). The cells were inoculated at a density of 0.5 x 10^6 cells ml^{-1} in 50 ml of RPMI 1640 supplemented with 10% FBS, 2mM L-Glutamine, 30 IU ml^{-1} IL-2 and 1:1 cells to Dynabeads® ratio. Following inoculation, a cap on the spinner flask arm was loosened in order to allow gas exchange. Medium was added on days 3 and 4, 10 and 40 ml respectively, after which the maximum working volume of 100 ml was reached.

ambr® 250 stirred-tank bioreactor culture

An 'ambr® 250 high throughput' two bioreactor test system (Sartorius Stedim Biotech, UK) was used for the studies, fitted with either of two types of single use bioreactors each of diameter, T = 60 mm. One vessel type, developed primarily for free suspension animal cell cultures, is equipped with two 3-segment, 30° pitched blade impellers (D = 26 mm) and 4 vertical baffles (width 6.25mm). The other vessel type, recently developed for microcarrier culture of adherent cell types, is equipped with a single larger 3-segment, 45° pitched blade impeller (D = 30mm) and is unbaffled (Figure 1). In both cases, the impellers pumped downwards and key culture parameters including pH, dO_2, temperature and the headspace gas flow were measured continuously and monitored throughout the experiment. T-175 Nunc™ non-treated flasks (ThermoFisher Scientific, UK) were used as a static control in parallel to the bioreactors and were placed in a humidified incubator at 37°C and 5% CO_2.

The ambr® 250 vessels were loaded and connected to the control system and 80 ml of RPMI 1640 with 10% FBS and 2mM L-Glutamine were placed in each vessel overnight in order to pre-condition the pH probe. 2 ml samples were taken from each vessel the following morning and the pH was also measured with an external pH probe for calibration. 5 x 10^7 human primary T-cells were then re-suspended in

22ml of RPMI 1640 supplemented with 10% FBS, 2mM L-Glutamine, 3000 IU IL-2, and 1:1 ratio of Dynabeads® for each vessel, reaching a final seeding density of $0.5x10^6$ cells ml^{-1} in a total volume of 100 ml. For each run, another 100 ml of complete RPMI 1640 supplemented with IL-2 was added on culture day 3 and a further 50 ml were added on day 4. A medium exchange was performed on day 5, stopping the impeller for 6 hours and removing 100ml of supernatant, and replacing it with fresh RPMI 1640 and IL-2. The medium addition/exchange strategy in the in the T-175 flasks mimicked that of the ambr250® bioreactors. The impeller agitation speeds used in the different runs for the ambr® 250 stirred-tank bioreactor studies are listed in Table 1 in which the volume changes are also illustrated. T-cells isolated from three different healthy donors (HD7, HD8 and HD12) were run separately across the different vessels at different speeds (Runs 1-4). Given how little has been done on cultivating T-cells in stirred bioreactors and the perception of 'shear sensitivity', the initial run was undertaken at the lowest speed available in the ambr® 250 designed for free suspension cell culture. Subsequent conditions were selected based on the result of the preceding run as discussed in the Results.

Oxygen was provided for cultivation by headspace aeration with the headspace flow regulated to 14.25 ml min^{-1} of N_2, with 21% O_2 and with an additional flow of CO_2 of 0.75 ml min^{-1}, in order to replicate the 5% CO_2 condition inside the incubator, used as the static control. Up until the medium exchange on day 5, dO_2 was generally above 60% as discussed later; after that time it was controlled at 60 % by gas blending with oxygen; 60% dO_2 being a typical value for free suspension cell culture (Nienow, 2015).

Separately, the power input was measured over a range of speeds using the same electrical technique as that used previously for characterising the ambr®15 bioreactor (Nienow et al., 2013a). A separate publication of these recent studies on multiple impeller configurations in the ambr® 250 is in preparation. These measurements gave a power number of 0.7 and 1.4 for the single and double pitched blade impellers respectively in the baffled vessel, and 2.1 for the single larger impeller in the unbaffled vessel.

Analytical techniques

A 1 ml sample was taken every day from each vessel and put into an Eppendorf tube in order to measure cell density and viability with the NucleoCounter® NC-3000™ (ChemoMetec A/S©, Denmark) using Via 1-Cassette™ (ChemoMetec A/S©, Denmark) containing acridine orange and DAPI. The same sample was then analysed with the CuBiAn HT270 bioanalyser (Optocell GmbH & Co, KG, Germany) in order to obtain glucose, ammonia and lactate concentrations. On the days, when a medium addition or exchange was performed, samples for metabolites concentration were taken before and after the fresh medium addition.

Once the metabolite data and viable cell number were collected, specific growth rate, doubling time, fold increase and specific metabolite consumption rate were determined.

Specific growth rate

$$\mu = \frac{(\ln\left(\frac{Cx(t)}{Cx(0)}\right))}{\Delta t}$$

Doubling time

$$t_d = \frac{ln_2}{\mu}$$

Fold expansion

$$FE = \frac{final\ viable\ cell\ numer}{initial\ viable\ cell\ number}$$

Specific consumption rate

$$q_{met} = \frac{\mu}{Cx(0)} * \frac{C_{met(t)} - C_{met(0)}}{e^{\mu t} - 1}$$

Lactate yield from glucose

$$\frac{Y_{Lac}}{Glc} = \frac{\Delta[Lac]}{\Delta[Glc]}$$

where

μ = specific growth rate [h^{-1}]

Cx(t) = the cell number at the end of the exponential growth phase [cells]

Cx(0) = cell number at the start of the exponential growth phase [cells]

Δt = duration of the exponential phase [h]

t_d = doubling time [h]

FE = fold expansion

q_{met} = specific consumption rate

$C_{met(t)}$ = metabolite concentration at the start of the exponential growth phase [mmol ml^{-1}]

$C_{met(0)}$ = metabolite concentration at the end of the exponential growth phase [mmol ml^{-1}]

t = time [h]

Y_{Lac}/Glc = lactate yield form glucose

Δ[Lac] = lactate production over a specific time period

Δ[Glc] = glucose consumption over the same time period

Immunophenotype

Phenotype analysis of the human primary T-cells was determined by flow cytometry after 7 days pre-expansion in T-Flask and at the end of the bioreactor culture, 7 days after inoculation. This was performed using BD LSRFortessa X-20 flow cytometer (BD Biosciences, UK) with 5 different lasers with

excitation at 355nm, 405nm, 488nm, 561nm and 640nm. The T-cells, both pre-expansion and post-harvest, were stained with the following antibodies; CD3-BUV396, CD4-FITC, CD8-BUV737, CD197 (CCR7)-BV421 and CD45RO-PE-Cy7 (BD Biosciences, UK). Cells were incubated in the fridge at 4°C for 30 minutes. Staining specificity was confirmed using fluorescence minus one (FMO) controls for CCR7 and CD45RO for each sample. The gating strategy for the immunophenotypic analysis is provided in Supplementary Figure 1. The cells were then washed with Stain Buffer (FBS) (BD Pharmingen™, BD Biosciences, UK) supernatant was removed and the cells were fixed using a 1X Phosphate Saline Buffer (PBS) solution (Thermo Fisher Scientific, UK) containing 4% (v/v) paraformaldehyde (PFA) (Sigma-Aldrich Company Ltd, UK). After 15 minutes at 4°C, two final washes were performed and the tubes were kept in the fridge, wrapped in aluminium foil for no longer than 2 days, until flow cytometer analysis was performed. A minimum of 50,000 events were recorded for each sample and the data was analysed using FlowJo™ computer software (Treestar, USA).

Statistical analysis

Data analysis was performed using GraphPad Prism 7 software (GraphPad, La Jolla, USA). Results are represented as mean ± SD. A one-way ANOVA test was used and values were considered statistically significant when probability (P) values were equal or below 0.05 (*), 0.01(**), 0.001(***), or 0.0001 (****).

Results

T-cell growth kinetics in the culture platforms

The initial studies investigated the growth of the T-cells in the spinner flasks (Figure 2) which, in comparison to the static T-flask condition, did not lead to any significant growth, resulting in a final cell number after 7 days of 0.18×10^6 cells ml^{-1}. This experiment was then followed by studies in the ambr® 250 stirred-tank bioreactors at various agitation speeds as outlined in Section 2.3 and listed along with the volume changes in Table 1.

The growth, metabolite flux, pH and dO_2 data from the four ambr® 250 bioreactor runs over 7 days of culture are shown in Figures 3-5. In Run 1, the two-impeller, baffled vessel which is widely utilised for ambr® 250 CHO suspension culture (Xu et al., 2017) was used at the lowest possible agitation speed of 100 rpm. During the first three days of culture when the volume in the vessel was 100 ml, only the lower impeller was submerged in the culture medium; after the 100 ml medium addition on day 3, both impellers were submerged. These conditions resulted in a final cell density $0.91 \pm 0.07 \times 10^6$ viable cells ml^{-1} which was significantly lower than the $2.38 \pm 0.25 \times 10^6$ viable cells ml^{-1} obtained for the static T-flask control (Figure 3a).

Another common perception is that the region near the baffles in baffled bioreactors is one of 'high shear' which is not present if baffles are not installed. Therefore, it was decided investigate the use of the new single impeller, unbaffled ambr® 250 vessel configuration, again using the lowest speed possible and the same culture parameters (Run 2). These conditions resulted in a higher final cell density of $3.62 \pm 0.23 \times 10^6$ viable cells ml^{-1} (Figure 3a). It seemed likely that it was the change in the fluid dynamic environment which resulted in the improved performance in Run 2 compared to Run 1 and to the T-flask.

However, there were two differences between the fluid dynamic regimes in Run 1 and Run 2. Not only have the baffles been removed in Run 2, in addition, because the impeller diameter and power number were greater, so was the specific power input (P/M), which defines the small scale turbulence structure generally considered to impart the stress on cells in stirred bioreactors (Nienow, 1998). The specific power input increased from 3.1×10^{-4} W kg^{-1} in Run 1, to 9.3×10^{-4} W kg^{-1} in Run 2 (Figure 3b).

Therefore, Run 3 was carried out using a higher speed in the original two-impeller, baffled vessel (the same vessel as used in Run 1). The basis for the increase was to produce the same specific power input (9.3×10^{-4} W kg^{-1}) as that in the new single-impeller, unbaffled vessel when run at 100 rpm. This approach meant operating the two-impeller baffled vessel at 180 rpm for the initial stages of the culture (when the volume was 100 ml and only one impeller was covered) and then reducing to 145 rpm when the volume increased to 200 and then 250 ml during the latter stages of the culture when both impellers were covered. Culture under these conditions resulted in a final cell density of $3.34 \pm 0.37 \times 10^6$ viable cells ml^{-1} (Figure 3a) being achieved which was comparable to the cell density obtained with single-impeller, unbaffled vessel in Run 2 (Figure 3a), both of which were higher than the final cell density obtained in the static T-flask control (Figure 3a). This result suggested that the presence of the baffles was not the reason for the poorer performance in Run 1.

Given the increase in final cell density achieved with the higher agitation speed in Run 3 compared with Run 1, it was decided to increase the impeller agitation speed further to 200 rpm in the single-impeller unbaffled vessel (Run 4). configuration resulted in a specific power input of 74×10^{-4} W kg^{-1} (Figure 3b) which yielded the highest cell density of $4.65 \pm 0.24 \times 10^6$ viable cells ml^{-1} (Figure 3a and Figure 3b) obtained after the 7 day culture period.

The cell growth kinetics is further illustrated in Figure 3c where the fold increase of all conditions investigated are shown. Run 1 (two-impeller, baffled vessel at 100 rpm) resulted in a significantly lower ($p<0.0005$) fold expansion at the harvest point (4.58 ± 0.329) compared with all the other expansion systems tested (Figure 3c). Both Run 2 (single-impeller, unbaffled vessel at 100 rpm) and Run 3 (two-impeller, baffled vessel at 180/145rpm) resulted in a higher fold expansion of 18.1 ± 1.2 and 17.1 ± 1.7 respectively in comparison with the T-flask control. Given the highest final cell density was achieved Run 4 (single-impeller unbaffled vessel at 200 rpm), this condition shows the greatest fold expansion of 23.2 ± 1.3 which is significantly larger ($p<0.0005$) than that of the T-flask static control which yielded a fold expansion of 15.2 ± 3.1.

In order to assess the inter-donor reproducibility, each donor was analysed separately and normalised to its own T-175 flask fold expansion (Figure 3d). All the conditions, except the baffled vessel at 100 rpm (0.39 ± 0.03), performed better than the T-Flask (reference line at normalised fold expansion = 1), as illustrated in Figure 3d. This analysis also demonstrated a high reproducibility between the 3 donors in all the systems tested, with the higher coefficient of variation (% CV) being 9.70% in Run 3 (baffled vessel at 180/145 rpm) (Figure 3d).

pH and dissolved oxygen concentrations

The pH and dO_2 were monitored throughout the duration of the 7 days expansion with the ambr® software (Figure 4). The spikes observed in the dO_2 profiles are due to the feeding of the system, which required the opening of the cap of the bioreactor (which was housed in a BSC). For all runs, the impeller was stopped on day 5 for 6 hours, in order to let the cells sediment and allow a 100 ml medium exchange, after which a dO_2 control at 60% was started (Figure 4).

The two-impeller baffled vessel at 100 rpm (Run 1) displayed a rapid lowering of the dO_2 (from 80 to 60%) when compared with the other runs (Figure 4a). This drop was probably because of the very low k_La at such a low agitation intensity. The dO_2 then increased to ~75%, perhaps because of cell death during the adaptation period so that the oxygen demand of the cells could be met, and then remained stable up to day 5 since cell numbers hardly increase. Agitation was then stopped and dO_2 fell to zero upon restarting, it was controlled at 60% by gas blending. This last sequence occurred in every run.

The starting dO_2 in all Runs 2-4 was ~90% and it remained stable for the first three days with the agitation intensity leading to a k_La seemingly matching the oxygen demand. After more medium was added and steady cell growth from day 3 to day 5, the oxygen demand of the cells could no longer be met and a drop occurred to dO_2~ 40% in Run 2 (Figure 4b), to 20% in Run 3 (Figure 4c) and to 50% in Run 4 (Figure 4d).

The pH profiles (Figure 4) correlates with the viable cell concentration (Figure 3a) and with the lactate production and accumulation (Figure 5b) as discussed below. The spikes in the pH measurements are due to medium addition and exchange (Figure 3). The pH readings in Run 1 (two-impeller baffled vessel at 100 rpm) showed higher readings compared to the other conditions, due to the lower number of viable cells in the system (Figure 3a). Runs 2 and 4 (single-impeller unbaffled vessel conditions at 100 and 200 rpm respectively) (Figure 3c and 3d) showed minimal differences in terms of pH profile, with the lower point being ~ 6.5 on day 3 and 5. Finally, the slope of the pH profile in the last hours of the cell culture for Run 3 (two-impeller baffled vessel at 180/145 rpm) and Run 4 (unbaffled vessel at 200 rpm) (Figure 4b and 4d) may indicate that the cell expansion slowed during this period.

Metabolite concentrations

The levels of glucose, lactate and ammonia were measured off-line on a daily basis (Figure 5). The glucose concentration (Figure 5a) reflects the trends previously described in terms of cell growth. The condition which resulted in the lowest final cell density (Run 1 – two-impeller baffled vessel 100 rpm) had the highest amount of glucose remaining in the medium samples (Figure 5a), correlating well with the cell growth kinetic data. The condition which resulted in the highest final cell density (Run 4 – single-impeller unbaffled vessel at 200 rpm), resulted in a lower glucose concentration in the medium when compared with the others.

The yield of lactate from glucose is presented in Figure 5d. The lowest value was found for Run 1 (single-impeller baffled vessel, 100rpm) which had an average value less than 1. However, there was no significant difference in the yield of lactate from glucose in all other conditions which resulted in values ranging from 1.51 ± 0.39 – 2.10 ± 0.58, which is close to 2 mol mol^{-1}, the maximum theoretical yield of lactate from glucose.

Assessment of cell quality

Flow cytometric analysis was performed at the beginning and at the end of the expansion in the bioreactors (Figure 6), with the CD4 to CD8 T cell ratio was taken as an indicator of the quality of the final product (Supplementary Figure 2). It can be seen from Figure 6b that the ratio of CD4:CD8 was higher at the beginning of the culture (4:1), while after the culture in the different systems, lowers towards the desired 1:1 value (Figure 6b). At the same time, a lower variability between the three different donors was shown after the expansion in the ambr® 250 stirred-tank bioreactor vessels compared to the T-flask static control. Moreover, the CD8+ T lymphocyte subpopulations were analysed in terms of naïve, central memory, effector memory and terminally differentiated T-cells. Figure 6c and 6d show CD8+ T central memory and effector memory subpopulation (the amount of naïve and terminally differentiated was lower than 5% in all samples). The central memory subpopulation was higher in the pre-experiment sample (62.61±10.58%) compared to the other conditions. On the other hand, the effector memory cells increased from 35.69±10.98% to ~ 80% after 7 days expansion in the different systems. Notably, no significant difference was found in the T-cell subpopulation profiles between the static T-flask control and the various ambr® 250 stirred-tank bioreactor runs.

Discussion

The interaction between agitation, Dynabeads® and cell growth

The initial run in the spinner flask, which did not result in any cell growth (Figure 2) would support the contention that T-cells are very 'shear sensitive'. However, careful observation of the spinner flask impeller, showed that most of the magnetic Dynabeads® were attached to it. The Dynabeads® have a magnetic core, as does the bar connected to the impeller paddle in the spinner flask, enabling the impeller paddle to be driven by a rotating magnet in the base. It would seem that because the Dynabeads® magnetically attached to the impeller spinner bar, the Dynabeads® were not well mixed in the culture vessel and did not interact effectively with the T-cells, which would be dispersed throughout the medium, leading to poor activation and, consequently, poor proliferation.

As discussed in the Results section above and as shown in Figure 3a, a poor result compared to the static T-flask control was also found in Run 1 when the baffled ambr® 250 bioreactor platform was used. This run was undertaken in the two-impeller baffled bioreactor vessel, which was originally developed for free suspension CHO culture. Due to the prevailing concerns regarding agitation speed and potential for fluid dynamic stresses on T-cells, the lowest possible agitation speed the system could accommodate was employed (100 rpm). At this point, it would have been easy to conclude that T-cells indeed prefer to be grown in static conditions and/or are very sensitive to fluid dynamic stress which was preventing growth. By persevering using the newer, larger diameter single-impeller in the unbaffled vessel (Run 2), a higher level of cell growth was obtained compared to both Run 1 and the T-flask. Run 3 in the baffled vessel and Run 4 in the unbaffled vessel, both at speeds higher than those used initially in the respective vessels, led to improved performance as shown in Figure 3a.

The fact that these increases in speed led to an improved performance in Run 2 compared to Run 1, and in Run 4 compared to Run 3, strongly suggests that the problems contributing to poor growth in Run 1 was due to some phenomenon other than fluid dynamic stress. One possibility is that at 100 rpm in Run 1, the Dynabeads® were not interacting with the cells due to poor suspension, resulting in inadequate T-cell activation. A key reason for this hypothesis is the poor performance in the spinner-flask where the magnetic core of the Dynabeads® was causing them to attach to the magnetic spinner rather than be fully suspended in the culture medium. In the T-flask, neither cells nor Dynabeads® are suspended, so that they are in contact even without motion. However, when Dynabeads® are not suspended and cells are, contact is very poor.

In addition, though the Dynabeads® are very small (a few microns in size) they are rather dense (SG ~ 1.4), much denser than microcarriers (SG < ~ 1.1). It is well established (Nienow, 1968; Zwietering, 1958) that the increase in speed required to just completely suspend particles (commonly designated as N_{JS}) of greater density is much higher than that required to accommodate particles of larger sizes. In addition, recent work has indicated that particles < ~ 15 μm require increasing speeds to suspend them compared to larger particles of about 80 μm (Janurin et al., 2018). The Dynabeads® are about ~4.5 μm in diameter. Thus, the relatively high density and the small size of the beads (which makes observation of suspension difficult) combine to suggest that at the lower agitation speed, the particles are not well suspended. This explanation for the poor performance in Run 1 is further reinforced by the improved performance with increased impeller speed for the two-impeller, baffled vessel in Run 3 and again for the unbaffled vessel between Run 2 and Run 4. Using multiple, identical donor material and consistent culture parameters with the exception of agitation speed, we observed a significant increase in the final cell density with increasing agitation.

Another parameter that suggests limited or poor activation of the cells is the lactate yield from glucose data (Figure 5d). Activated T-cells are known to require an increased source of energy in order to

proliferate, which is reflected in an increase in the uptake of glucose and production of lactate (Wahl et al., 2010). In this work, Run 1 (two impeller-baffled vessel at 100 rpm) resulted in the lowest mean value of lactate yield from glucose (Figure 5d), suggesting that the pyruvate produced maybe being used in oxidative phosphorylation rather than converted into lactate *via* glycolysis (Ozturk et al., 1997), and thereby suggesting a lack of activation.

The impact of agitated stirred-tank bioreactor culture on cell quality

Although it was demonstrated that primary human T-cells from multiple donors could be cultivated more effectively in an ambr® 250 stirred-tank bioreactor in comparison to a static T-flask control, it is necessary to take into account any impact on cell quality. This was ascertained by assessing cellular immunophenotype. CD4:CD8 T-cell ratio and CD8+ T-cell subpopulations were further analysed before inoculation and post-harvest in terms of the naïve, central memory, effector memory and terminally differentiated T-cells. With respect to the CD4:CD8 T cell ratio, ideally an equal amount of CD4 and CD8 T-cells would be present in the final composition (Turtle et al., 2016). From the data obtained, there was a greater level of consistency between replicates with Runs 2-4 in comparison to the static T-flask control. This difference may be indicative of the benefits of automation and improved process monitoring and control associated with automated bioreactor platforms as shown previously for human mesenchymal stem cell/microcarrier cultures in the ambr® 15 microbioreactor system (Rafiq et al., 2017).

Naïve and central memory T-cells have a higher persistence when reinfused into the patient (Sommermeyer et al., 2016), therefore a higher percentage of these cells and a lower percentage of T-cells in more differentiated stages are desirable in the final product for immunotherapy applications. Figure 6b and 6c show CD8+ T central memory and effector memory subpopulations (the amount of naïve and terminally differentiated was lower than 5% in all samples). Although the expanded cells appeared to have a more differentiated phenotype, importantly, this was the case irrespective of the culture platform or agitation conditions. The tendency of the cells to differentiate toward the effector memory phenotype can be explained by the prolonged expansion protocol (14 days in total including cell pre-expansion prior to bioreactor inoculation) and the use of IL-2 in the medium, which was shown to provoke differentiation if used for lengthy periods (Crompton et al., 2014). This data suggests that further optimization of the culture process (both static T-flask and stirred-tank bioreactor culture) is required to facilitate the production of the desired T-cell subset. However, with the potential for high-throughput development using systems like the ambr® 250 bioreactor, this investigation paves the way for design of experiment approaches to be used to streamline T-cell manufacturing optimization efforts. Importantly, cell differentiation was not impacted by the agitation regime, presenting a similar phenotype to the static controls, thereby suggesting that an agitated culture environment does not impact the cell differentiation, whilst achieving, in certain conditions, an increased fold expansion.

Comparison of agitation intensity (W kg^{-1}) and cell growth and quality

The presence of the magnetic field in the spinner flask and the magnetic core of the Dynabeads® clearly explains the attachment of the beads to the spinner stirrer bar and other surfaces. This attachment also is the reason for the poor culture performance in the spinner flask and it is not related in any way to the fluid dynamic environment present.

To make a comparison of, and explain the difference in the culture performance in the two configurations of the stirred ambr® 250 bioreactor vessel, where the only difference between the various runs was the fluid dynamic environments, it is helpful to compare the specific power input which is numerically equivalent to the mean specific energy dissipation rate. Indeed, these parameters are also

very important if comparison with the culture of other free suspension cells is to be made. The power input is given by Equation 1:

$$P = Po\rho N^3 D^5 \qquad 1$$

where P (W) is the power input, Po is the power number (dimensionless), ρ (kg m^{-3}) is the density of the medium (here assumed to have the same physical properties as water), N (rev s^{-1}) is the impeller speed and D (m) is the impeller diameter. The specific power is then P/M W kg^{-1} where M (kg) is the mass of medium in the bioreactor (Nienow, 1998) which in each run varies with time as described above. Table 1 also gives the various P/M values at the different stages of the 4 runs in the bioreactor.

In Run 1 (two-impeller baffled vessel operating at 100 rpm), P/M is very low, much lower than would normally be found in free suspension culture (Nienow, 2006). However, since the dO_2 does not drop below ~ 60%, the fact that the cells hardly grow cannot be attributed to inadequate mass transfer. At the higher speed in Run 3 (the baffled vessel), initially P/M = 2.2 x 10^{-3} W kg^{-1} (2.2 W m^{-3}), which is still low for free suspension culture but within the range used. Now, the cells grow relatively well, which certainly does not suggest that the problem at the lower speed was due to fluid dynamic stresses damaging cells. After the volume of medium in the bioreactor was increased and the speed reduced, the specific power initially remained the same because both impellers are contributing to P/M. However, after day 4, when the volume is increased again, the specific power and the specific upper surface area of the medium decreases and the rate of decrease of dO_2 significantly increases to reach a value ~ 20% at day 5, going back to 60% when dO_2 by gas blending kicks in (Figure 4). The higher rate of fall is due to the lower rate of O_2 mass transfer from the headspace and the increasing cell density at the latter stage of culture leading to a higher oxygen demand.

Comparing Runs 2 and 3, the P/M value tracks extremely closely between both runs, as indeed was the intention. As can be seen, in that case, all measured parameters in the majority of cases are remarkably similar (Figures 3- 5). In both cases, the culture performance is superior to that obtained in the static T-flask control.

In Run 4, the P/M value (74 x 10^{-4} W kg^{-1}) is typical of that found in commercial processes across many scales in free suspension culture (Nienow et al., 2013b) and the cell growth is the highest by a considerable margin (Figure 3b). Again, there is no indication of 'shear sensitivity'. To assess the likelihood of fluid dynamic stress damaging cells, the usual approach is to compare the size of the cell to that of the Kolmogorov scale of turbulence, λ_K (m), where

$$\lambda_K = (\varepsilon_{Tmax}/\upsilon^3)^{-1/4} \quad 2$$

where ε_{Tmax} (W kg^{-1}) is the maximum specific energy dissipation rate close to the impeller and υ (m^2 s^{-1}) is the kinematic viscosity. If λ_K > size of the cell, it should not be damaged. The precise value of the maximum to the mean specific energy dissipation rate (=P/M) has proved difficult to measure (Gabriele et al., 2009) but based on the literature, a reasonable but high value in order to assess the likelihood of damage can be assumed. Thus, assuming that ε_{Tmax} is 50 times the mean specific energy dissipation rate (= P/M) for the geometry in question (Nienow et al., 2016), then λ_K = 32 μm >> size of T-cell. Thus, damage would not be expected based on this analysis of the impact of turbulence on cells.

This discussion strengthens further the earlier suggestion that the reason for the poor performance at the lowest P/M, Run 1 (3.1 x 10^{-4} W kg^{-1}), was due to the inability of the agitation to suspend the Dynabeads®. Here it is shown that at the highest P/M investigated, Run 4 (74 x 10^{-4} W kg^{-1}), the Kolmogorov scale is greater than the size of the T-cell. It is also seen that the higher P/M, the better performance. It is worth noting in this instance, it was not a lack of oxygen transfer that prevented the cells growing at the lowest P/M, nor was dO_2 a problem at the higher speed. Higher speeds increase many mixing parameters but here we argue that the current results indicate that it is better cell-bead contact that gives the better performance. This relationship suggests that the interaction between Dynabeads® and cell is related to the frequency with which each is brought into contact with the other. Even though the Reynolds number here (~ 3000) at the highest P/M is less than the value at which turbulence is fully established, it has been found that analysis based on the assumption of turbulent flow works well for hMSCs grown on microcarriers at similar Reynolds numbers (Nienow et al., 2016). Under turbulent flow conditions, the higher the specific energy dissipation rate, the greater the rate of contact of particles (Davies, 1972; Levich, 1962), so the concept that higher P/M values lead to greater interaction between cells and Dynabeads® and improved culture seems reasonable. In addition, higher agitation intensity above the minimum required for suspension, N_{JS}, leads to a more homogeneous distribution of particles throughout the media (Nienow, 1997a), thus further improving the contact between Dynabeads® and cells.

At the moment, the precise mode of action in such environments is not well understood and requires more investigation. But the concept that impeller agitation damages T-cells preventing their culture in stirred-tank bioreactors is clearly incorrect. Even at the present agitation intensities when the beads are suspended, the interaction between beads and cells, and the homogeneity achieved by the agitation, is such that the performance in the stirred-tank bioreactors is better than in the T-flask whilst the cells after cultivation are essentially the same independently of the configuration used. The higher the agitation intensity used here the better the result; and the analysis of the Kolmogorov microscale suggests that even better results might be obtained with even higher agitation intensities by enhancing cell-Dynabeads® interactions without cell damage.

Conclusions

The focus of the study was to establish whether human primary T-cells could be cultured in stirred-tank bioreactor systems which have proven scalability and process control capability. There has been a general reticence to use such systems due to unsubstantiated concerns that T-cells grow better under static conditions (i.e. in T-flasks or cell culture bags) or that the potential fluid dynamic forces in a stirred-tank bioreactor system would impair the growth and/or function of T-cells. In this study, however, we demonstrate that not only can T-cells be cultured in stirred-tank bioreactors, but that higher impeller agitation speeds facilitate higher cell densities with no adverse impact on cell quality. Importantly, from the data obtained, there is no indication that T-cells prefer being grown under static conditions or are sensitive to fluid dynamic stresses within a stirred-tank bioreactor system at the agitation speeds investigated. Indeed, the opposite has proven to be the case, whereby the cells grow better under

higher agitation speeds, and in all but one investigation (Run 1), result in a higher final cell density compared to the T-flask static control where dO_2 control could not be used.

Acknowledgements

The authors would like to acknowledge the funding and support of the UK Engineering and Physical Sciences Research Council (EPSRC) through the Future Targeted Healthcare Manufacturing Hub hosted at University College London with UK university partners (Grant Reference: EP/P006485/1) and includes financial and in-kind support from the consortium of industrial users and sector organisations. Funding and support from the EPSRC CDT Bioprocess Engineering Leadership (Grant Number: EP/L01520X/1) and the EPSRC New Industrial Systems: Optimising Me Manufacturing Systems grant (Grant Number: EP/R022534/1) are also acknowledged.

References

Alliance for Regenerative Medicine. (2018). The Alliance for Regenerative Medicine Releases Q3 2018 Data Report, Highlighting Sector Trends and Metrics. Retrieved from https://alliancerm.org/publication/q3-2018-data-report/

Badenes, S. M., Fernandes, T. G., Miranda, C. C., Pusch-Klein, A., Haupt, S., Rodrigues, C. A. V., . . . Cabral, J. M. S. (2017). Long-term expansion of human induced pluripotent stem cells in a microcarrier-based dynamic system. *Journal of Chemical Technology & Biotechnology, 92*(3), 492-503. doi:10.1002/jctb.5074

BioPharma Dive. (2018). In CAR-T, manufacturing a hurdle Novartis has yet to clear. Retrieved from https://www.biopharmadive.com/news/in-car-t-manufacturing-a-hurdle-novartis-has-yet-to-clear/543624/

Bohnenkamp, H., Hilbert, U.& Noll T. (2002) Bioprocess development for the cultivation of human T-lymphocytes in a clinical scale. *Cytotechnology.* 38(1-3); 135–145. doi:10.1023/A:1021174619613

Business Insider. (2018). A cutting-edge new cancer treatment has two different price tags, and it could be the future of how we pay for drugs. Retrieved from https://www.businessinsider.com/indication-based-pricing-for-novartis-car-t-cell-therapy-kymriah-2018-5?r=UK&IR=T

Carmelo, J. G., Fernandes-Platzgummer, A., Cabral, J. M., & da Silva, C. L. (2015). Scalable ex vivo expansion of human mesenchymal stem/stromal cells in microcarrier-based stirred culture systems. *Methods in Molecular Biology, 1283*, 147-159. doi:10.1007/7651_2014_100

Carswell, K. S. & Papoutsakis, E.T. (2000) Culture of human T cells in stirred bioreactors for cellular immunotherapy applications: shear, proliferation, and the IL-2 receptor. *Biotechnology and Bioengineering* 68(3):328-38.

Celyad. (2018). Celyad Announces FDA Acceptance of IND Application for CYAD-101, a First-in-Class Non-Gene Edited Allogeneic CAR-T Candidate. Retrieved from https://www.celyad.com/en/news/celyad-announces-fda-acceptance-of-ind-application-for-cyad-101-a-first-in-class-non-gene-edited-allogeneic-car-t-candidate

Chen, A. K., Chew, Y. K., Tan, H. Y., Reuveny, S., & Weng Oh, S. K. (2015). Increasing efficiency of human mesenchymal stromal cell culture by optimization of microcarrier concentration and design of medium feed. *Cytotherapy, 17*(2), 163-173. doi:10.1016/j.jcyt.2014.08.011

Crompton, J. G., Sukumar, M., & Restifo, N. P. (2014). Uncoupling T-cell expansion from effector differentiation in cell-based immunotherapy. *Immunological Reviews, 257*(1), 264-276. doi:10.1111/imr.12135

Davies, J. T. (1972). *Turbulence Phenomena*. London: Academic Press.

Diogo, M. M., Miranda, C. C., Fernandes, T. G., Pascoal, J. F., & Cabral, J. M. S. (2015, January). *Temporal and spatial control of the neural commitment of human pluripotent stem cells as suspension aggregates.* Paper presented at the Scale-up and manufacturing of cell based therapies IV, San Diego, California.

EMA. (2018a). EMA Approved Products - Kymriah. Retrieved from https://www.ema.europa.eu/en/medicines/human/EPAR/kymriah

EMA. (2018b). EMA Approved Products - Yescarta. Retrieved from https://www.ema.europa.eu/medicines/human/EPAR/yescarta

EMA. (2018c). New gene therapy for rare inherited disorder causing vision loss recommended for approval. Retrieved from https://www.ema.europa.eu/en/news/new-gene-therapy-rare-inherited-disorder-causing-vision-loss-recommended-approval

FDA. (2019). Approved Cellular and Gene Therapy Products. Retrieved from https://www.fda.gov/BiologicsBloodVaccines/CellularGeneTherapyProducts/ApprovedProducts/default.htm

Gabriele, A., Nienow, A. W., & Simmons, M. J. H. (2009). Use of angle resolved PIV to estimate local specific energy dissipation rates for up- and down-pumping pitched blade agitators in a stirred tank. *Chemical Engineering Science, 64*(1), 126-143. doi:http://dx.doi.org/10.1016/j.ces.2008.09.018

Gouble, A., Philip, B., Poirot, L., Schiffer-Mannioui, C., Galetto, R., Derniame, S., . . . Smith, J. (2014). In Vivo Proof of Concept of Activity and Safety of UCART19, an Allogeneic “Off-the-Shelf” Adoptive T-Cell Immunotherapy Against CD19⁺ B-Cell Leukemias. *Blood, 124*(21), 4689.

Heathman, T. R. J., Glyn, V. A. M., Picken, A., Rafiq, Q. A., Coopman, K., Nienow, A. W., . . . Hewitt, C. J. (2015). Expansion, harvest and cryopreservation of human mesenchymal stem cells in a serum-free microcarrier process. *Biotechnology and Bioengineering, 112*(8), 1696-1707. doi:10.1002/bit.25582

Hewitt, C. J., Lee, K., Nienow, A. W., Thomas, R. J., Smith, M., & Thomas, C. R. (2011). Expansion of human mesenchymal stem cells on microcarriers. *Biotechnology Letters, 33*(11), 2325-2335. doi:10.1007/s10529-011-0695-4

Janurin, N. S., Choong, C. E., Zimzam, Z., & Ibrahim, S. (2018). *Suspension Characteristics of Fine Particles at High Loadings in Flat and Dished Base Tanks*. Paper presented at the 16th European Mixing conference on Mixing, Toulouse, France.

Klarer, A., Smith, D., Cassidy, R., Heathman, T. R. J., & Rafiq, Q. A. (2018). Demonstrating scalable T-cell expansion in stirred-tank bioreactors. *Bioprocess International, 16*(6), 6-14.

Levich, V. G. (1962). *Physicochemical Hydrodynamics*. Englewood Cliffs: Prentice-Hall.

Marsh, D. T. J., Lye, G. J., Micheletti, M., Odeleye, A. O. O., Ducci, A., & Osborne, M. D. (2017). Fluid dynamic characterization of a laboratory scale rocked bag bioreactor. *AIChE Journal, 63*(9), 4177-4187. doi:10.1002/aic.15734

NHS England. (2018). NHS England strikes deal for ground breaking cancer treatment in a new European first. Retrieved from https://www.england.nhs.uk/2018/10/nhs-england-strikes-deal-for-ground-breaking-cancer-treatment-in-a-new-european-first/

Nienow, A. W. (1968). Suspension of solid particles in turbine agitated baffled vessels. *Chemical Engineering Science, 23*(12), 1453-1459. doi:https://doi.org/10.1016/0009-2509(68)89055-4

Nienow, A. W. (1997). The suspension of solid particles. In: *Mixing in the Process Industries*, 2nd Edition (paperback revision), (Editors, N. Harnby, M.F. Edwards and A.W. Nienow), Butterworth Heinemann, London, Chapter 16, pp.364-393.

Nienow, A. W. (1998). Hydrodynamics of stirred bioreactors. *Applied Mechanics Reviews, 51*(1), 3-32. doi:10.1115/1.3098990

Nienow, A. W. (2006). Reactor engineering in large scale animal cell culture. *Cytotechnology, 50*(1-3), 9-33. doi:10.1007/s10616-006-9005-8

Nienow, A. W. (2015). Mass Transfer and Mixing Across the Scales in Animal Cell Culture. In M. Al-Rubeai (Ed.), *Animal Cell Culture* (Vol. 9, pp. 137-167): Springer International Publishing.

Nienow, A. W., Hewitt, C. J., Heathman, T. R. J., Glyn, V. A. M., Fonte, G. N., Hanga, M. P., . . . Rafiq, Q. A. (2016). Agitation conditions for the culture and detachment of hMSCs from microcarriers in multiple bioreactor platforms. *Biochemical Engineering Journal, 108*, 24-29. doi:http://dx.doi.org/10.1016/j.bej.2015.08.003

Nienow, A. W., Rafiq, Q. A., Coopman, K., & Hewitt, C. J. (2014). A potentially scalable method for the harvesting of hMSCs from microcarriers. *Biochemical Engineering Journal, 85*(0), 79-88. doi:http://dx.doi.org/10.1016/j.bej.2014.02.005

Nienow, A. W., Rielly, C. D., Brosnan, K., Bargh, N., Lee, K., Coopman, K., & Hewitt, C. J. (2013a). The physical characterisation of a microscale parallel bioreactor platform with an industrial CHO cell line expressing an IgG4. *Biochemical Engineering Journal, 76*(0), 25-36. doi:http://dx.doi.org/10.1016/j.bej.2013.04.011

Nienow, A. W., Scott, W. H., Hewitt, C. J., Thomas, C. R., Lewis, G., Amanullah, A., . . . Meier, S. J. (2013b). Scale-down studies for assessing the impact of different stress parameters on growth and product quality during animal cell culture. *Chemical Engineering Research and Design, 91*(11), 2265-2274.

Ozturk, S. S., Jorjani, P., Taticek, R., Lowe, B., Shackleford, S., Ladehoff-Guiles, D., . . . Naveh, D. (1997). Kinetics of Glucose Metabolism and Utilization of Lactate in Mammalian Cell Cultures. In M. J. T. Carrondo, B. Griffiths, & J. L. P. Moreira (Eds.), *Animal Cell Technology: From Vaccines to Genetic Medicine* (pp. 355-360). Dordrecht: Springer Netherlands.

Rafiq, Q. A., Brosnan, K. M., Coopman, K., Nienow, A. W., & Hewitt, C. J. (2013a). Culture of human mesenchymal stem cells on microcarriers in a 5 l stirred-tank bioreactor. *Biotechnology Letters, 35*(8), 1233-1245. doi:10.1007/s10529-013-1211-9

Rafiq, Q. A., Coopman, K., & Hewitt, C. J. (2013b). Scale-up of human mesenchymal stem cell culture: current technologies and future challenges. *Current Opinion in Chemical Engineering, 2*(1), 8-16. doi:http://dx.doi.org/10.1016/j.coche.2013.01.005

Rafiq, Q. A., Coopman, K., Nienow, A. W., & Hewitt, C. J. (2013c). A quantitative approach for understanding small-scale human mesenchymal stem cell culture - implications for large-scale bioprocess development. *Biotechnology Journal, 8*(4), 459-471. doi:10.1002/biot.201200197

Rafiq, Q. A., Coopman, K., Nienow, A. W., & Hewitt, C. J. (2016a). Systematic microcarrier screening and agitated culture conditions improves human mesenchymal stem cell yield in bioreactors. *Biotechnology Journal, 11*(4), 473-486. doi:10.1002/biot.201400862

Rafiq, Q. A., Hanga, M. P., Heathman, T. R. J., Coopman, K., Nienow, A. W., Williams, D. J., & Hewitt, C. J. (2017). Process development of human multipotent stromal cell microcarrier culture using an automated high-throughput microbioreactor. *Biotechnology and Bioengineering, 114*(10), 2253-2266. doi:10.1002/bit.26359

Rafiq, Q. A., Heathman, T. R. J., Coopman, K., Nienow, A. W., & Hewitt, C. J. (2016b). Scalable Manufacture for Cell Therapy Needs. In *Bioreactors* (pp. 113-146): Wiley-VCH Verlag GmbH & Co. KGaA.

Rafiq, Q. A., & Hewitt, C. J. (2015). Cell therapies: why scale matters. *Pharmaceutical Bioprocessing, 3*(2), 97-99. doi:10.4155/pbp.14.63

Sommermeyer, D., Hudecek, M., Kosasih, P. L., Gogishvili, T., Maloney, D. G., Turtle, C. J., & Riddell, S. R. (2016). Chimeric antigen receptor-modified T cells derived from defined CD8+ and CD4+ subsets confer superior antitumor reactivity in vivo. *Leukemia, 30*(2), 492-500. doi:10.1038/leu.2015.247

Turtle, C. J., Hanafi, L. A., Berger, C., Gooley, T. A., Cherian, S., Hudecek, M., . . . Maloney, D. G. (2016). CD19 CAR-T cells of defined CD4+:CD8+ composition in adult B cell ALL patients. *Journal of Clinical Investigation, 126*(6), 2123-2138. doi:10.1172/jci85309

Vormittag, P., Gunn, R., Ghorashian, S., & Veraitch, F. S. (2018). A guide to manufacturing CAR T cell therapies. *Current Opinion in Biotechnology, 53*, 164-181. doi:https://doi.org/10.1016/j.copbio.2018.01.025

Wahl, D. R., Petersen, B., Warner, R., Richardson, B. C., Glick, G. D., & Opipari, A. W. (2010). Characterization of the metabolic phenotype of chronically activated lymphocytes. *Lupus, 19*(13), 1492-1501. doi:10.1177/0961203310373109

Wang, X., & Rivière, I. (2016). Clinical manufacturing of CAR T cells: foundation of a promising therapy. *Molecular therapy oncolytics, 3*, 16015-16015. doi:10.1038/mto.2016.15

Xu, P., Clark, C., Ryder, T., Sparks, C., Zhou, J., Wang, M., . . . Scott, C. (2017). Characterization of TAP Ambr 250 disposable bioreactors, as a reliable scale-down model for biologics process development. *Biotechnology Progress, 33*(2), 478-489. doi:doi:10.1002/btpr.2417

Zwietering, T. N. (1958). Suspending of solid particles in liquid by agitators. *Chemical Engineering Science, 8*(3–4), 244-253. doi:http://dx.doi.org/10.1016/0009-2509(58)85031-9

Figures

Figure 1: ambr® 250 baffled (top) and unbaffled (bottom) vessels. The baffled vessel has two 3-segment, 30° pitched blade impellers and 4 vertical baffles. The unbaffled vessel has a single 3-segment, 45° pitched blade impeller and no baffles. T=diameter of the vessel (60 mm), D=diameter of the impeller, C=impeller height from bottom and W=baffle width.

Baffled Vessel		
Impeller diameter (3-pitched blade) (D)	26 mm	T/D = 2.3
Impeller height from bottom (C)	17 mm	C/D = 0.65
Impeller number	2	
Impeller spacing	30 mm	
No. of baffles	4	
Baffle width (W)	6.25 mm	W/T = 0.1

Baffled Vessel (two impellers)

Unbaffled Vessel		
Impeller diameter (Elephant ear) (D)	30 mm	T/D = 2
Impeller height from bottom (C)	17 mm	C/D = 0.56
Impeller number	1	
No. of baffles	0	

Unbaffled Vessel (single impeller)

Figure 2: The growth of primary T-cells in static T-175 flasks (n=3) and in a spinner flask (n=1) at 35 rpm over 7 days. The black arrows indicate the media addition for both systems on day 3 (20 ml in the T-175 flask and 10 ml in the spinner flask) and day 4 (10 ml in the T-175 flask and 40 ml in the spinner flask), while the black arrow on day 5 indicates a media addition for the T-175 flask only. Data for the T-175 flask shown as mean ± SD.

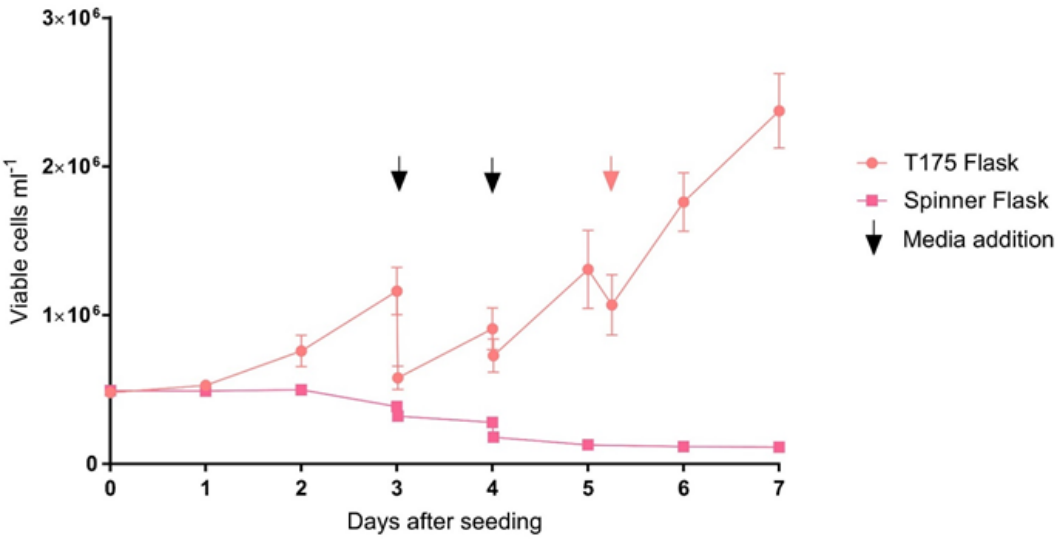

Figure 3: The growth of primary T-cells from multiple donors over 7 days in T-175 flask (n=3) and under different agitation and fill conditions in the two ambr® 250 vessels (n=3. a) Viable cell density (cells ml^{-1}). The black arrow indicates a medium addition on days 3 (200 ml) and 4 (100 ml) and a medium exchange (100 ml) on day 5. Data shows mean ± SD. b) Final viable cell density (cells ml^{-1}) at day 7 plotted against the specific power input (W kg^{-1} x 10^{-4}) at the end of each run. Data shown as mean ± SD. c) Fold expansion (total number of viable cells at day 7/total number of viable cells at seeding). Data shown as mean ± SD. d) Fold expansion for each donor (HD7, HD8 and HD12) in the ambr® 250 cultures normalised with the fold expansion for the same donor in T-175 flasks. The reference dotted line at 1 shows the equivalence in fold expansion between the static control (T-175 flask) and the condition tested. Statistical significance is shown when probability (P) values were equal or below 0.05 (*), 0.01(**), 0.001(***), or 0.0001 (****).

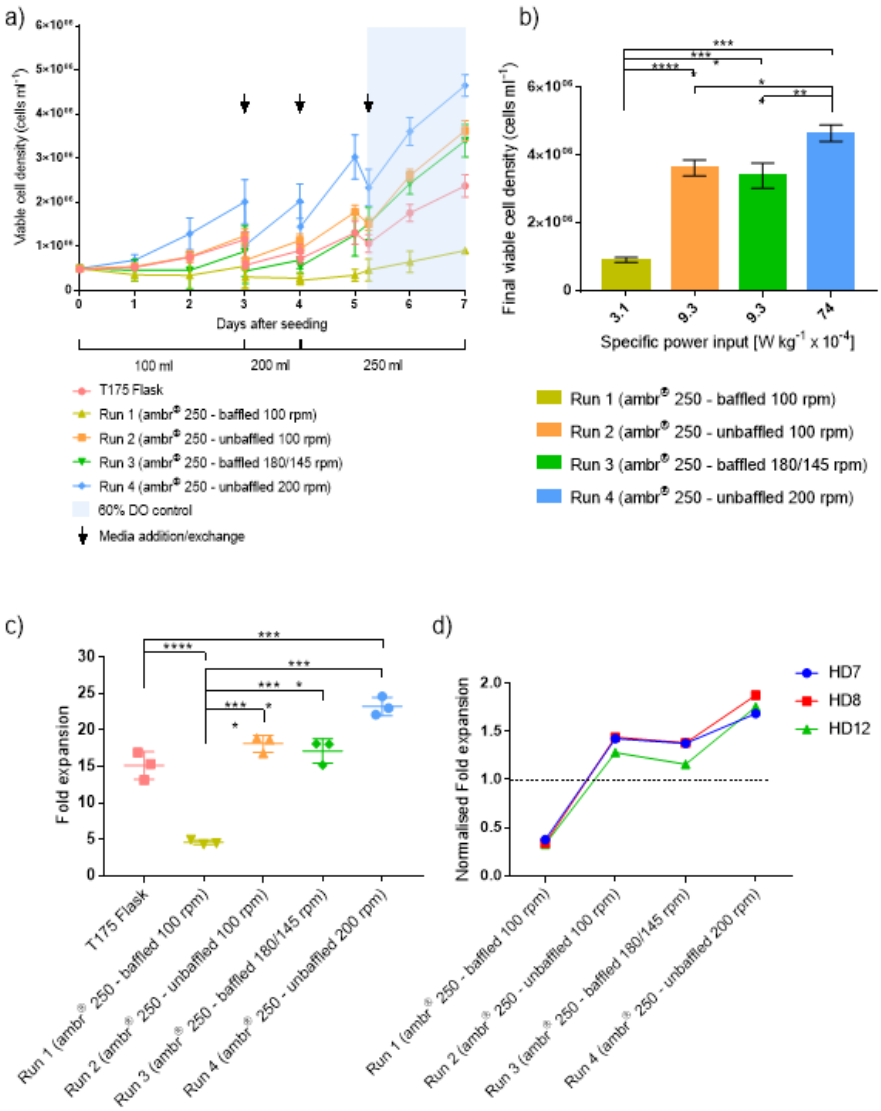

Figure 4: Representative dissolved oxygen (dO_2) (left hand side) and pH (right hand side) trends under different agitation and fill conditions in the two ambr® 250 vessels over 7 days. In all runs, dO_2 control at 60% was introduced at day 5 after the impeller was stopped for 6 hours (dO_2 at 0%) in order to let the cells sediment and perform a 100ml media exchange. a) Run 1 – in the baffled vessel at 100 rpm. b) Run 2 – in the unbaffled vessel at 100 rpm. c) Run 3 – in the baffled vessel at 180/145 rpm (the speed was changed on day 3) d) Run 4 – in the unbaffled vessel at 200 rpm.

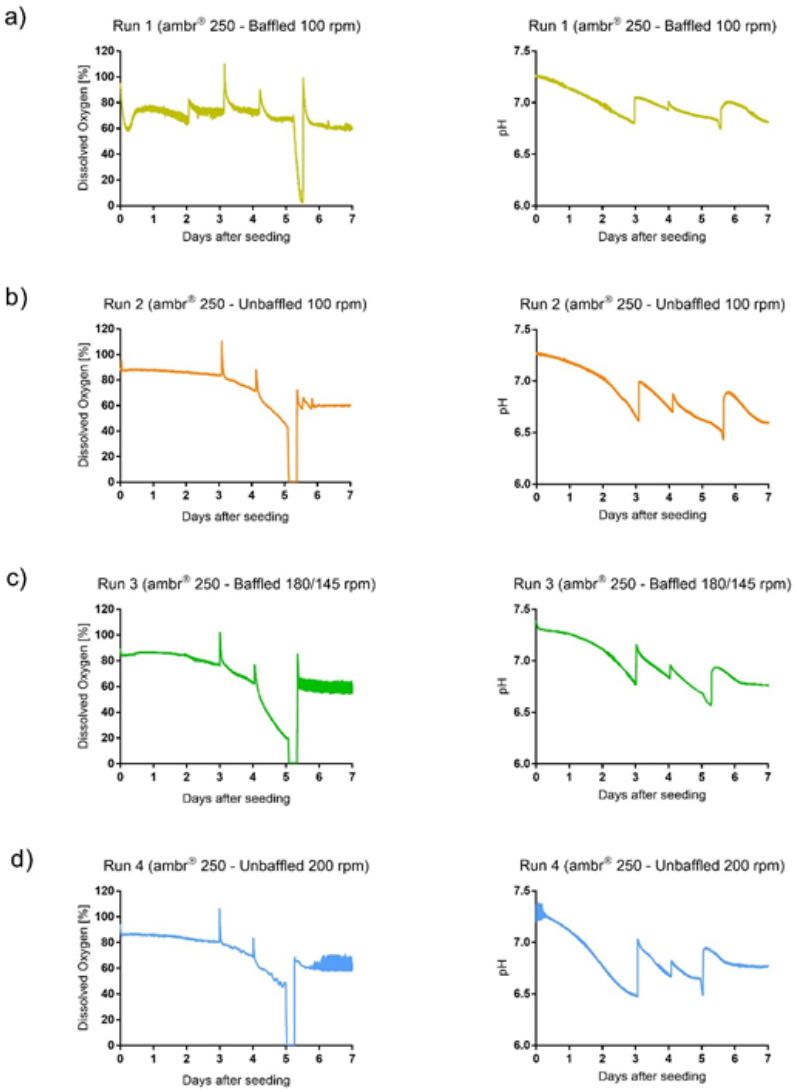

Figure 5: Metabolite concentration profiles under the different agitation and fill conditions in the two ambr® 250 vessels over 7 days and in T175 Flasks as a static control. The black arrows indicate a media addition/exchange. Data shows mean ± SD, n=3. a) Glucose concentration in the media from day 0 to the end of the expansion. b) Lactate concentration in the culture media in all the examined conditions. c) Ammonia concentration in the culture media in the different expansion systems. d) Yields of lactate from glucose. Reference line at 2 is the maximum theoretical yield of lactate from glucose.

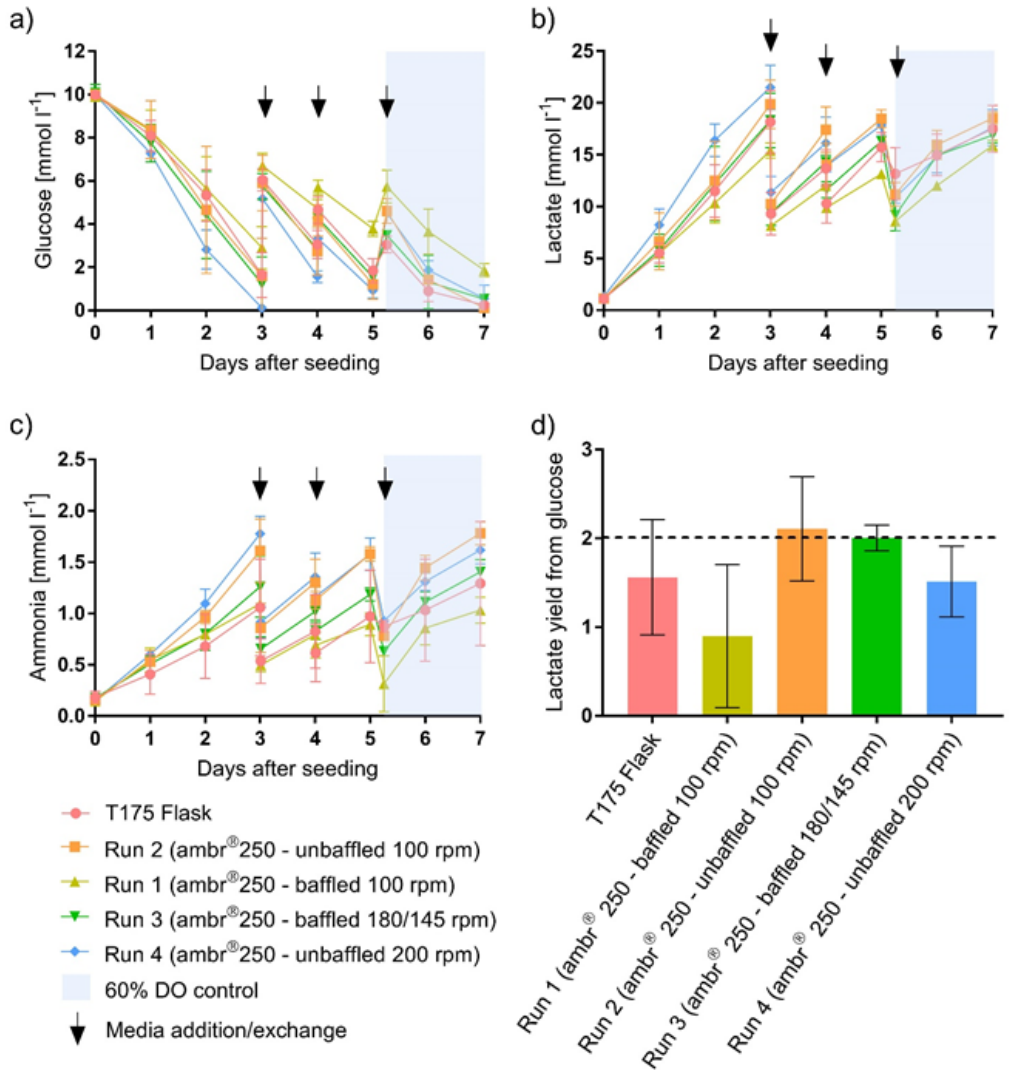

Figure 6: Phenotypic characterisation of primary T-cells when seeded in the bioreactor (pre-experiment - black) and post-harvest in the different agitation and fill conditions in the two ambr® 250 vessels over 7 days and in T175 Flasks as a static control. Data shows mean ± SD. a) Sample gating strategy showing single cells gating, CD3 positive cells, CD4 and CD8+ T cells and finally the CD8+ T cell subpopulations gated based on FMO controls. b) CD4 to CD8 T cell ratio c) CD8+ T central memory (CCR7+ CD45RO+) subpopulation percentage of the cells. d) CD8+ T effector memory (CCR7- CD45RO+) subpopulation percentage in all the analysed conditions compare to the pre-experiment sample.

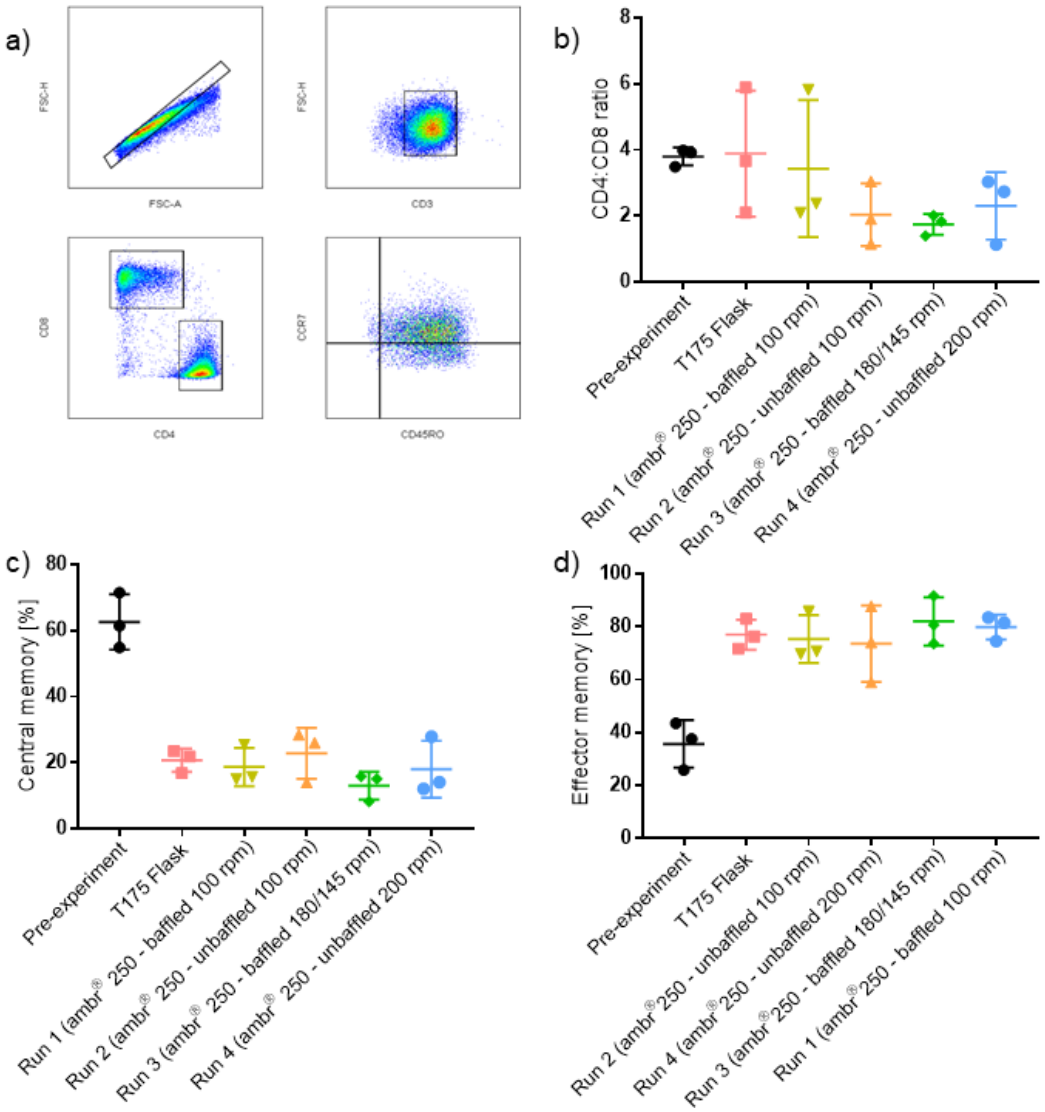

TABLE

Table 1: Different conditions tested in the ambr® bioreactors, each indicating the working volumes, number of impellers submerged by the media and correspondent speed and specific power input at different times throughout the experiments.

	Run 1	Run 2	Run 3	Run 4
Vessel type	*Baffled (two impellers)*	*Unbaffled (single impeller)*	*Baffled (two impellers)*	*Unbaffled (single impeller)*
Starting volume day 1-3		100 ml		
Impeller agitation speed (rpm) / x 10^{-4} W kg^{-1} from day 1-3	100/3.8	100/23	180/22	200/184
Number of impellers submerged in the culture medium day 1-3	1	1	1	1
Working volume day 3 - 4		200 ml		
Impeller agitation speed (rpm) / x 10^{-4} W kg^{-1} from day 3 - 4	100/3.8	100/12	145/12	200/92
Number of impellers submerged by the culture medium day 3-4	2	1	2	1
Working volume day 4 - 7		250 ml		
Impeller agitation speed (rpm) / x 10^{-4} W kg^{-1} from day 4-7	100/3.1	100/9.3	145/9.3	200/74
Number of impellers submerged by the culture medium day 4-7	2	1	2	1